

Quantum frequency up-conversion of continuous variable entangled states

Wenyuan Liu, Ning Wang, Zongyang Li, and Yongmin Li^{a)}

State Key Laboratory of Quantum Optics and Quantum Optics Devices, Institute of Opto-Electronics, Shanxi University, Taiyuan 030006, China

(Received 25 September 2015; accepted 29 November 2015; published online 10 December 2015)

We demonstrate experimentally quantum frequency up-conversion of a continuous variable entangled optical field via sum-frequency-generation process. The two-color entangled state initially entangled at 806 and 1518 nm with an amplitude quadrature difference squeezing of 3.2 dB and phase quadrature sum squeezing of 3.1 dB is converted to a new entangled state at 530 and 1518 nm with the amplitude quadrature difference squeezing of 1.7 dB and phase quadrature sum squeezing of 1.8 dB. Our implementation enables the observation of entanglement between two light fields spanning approximately 1.5 octaves in optical frequency. The presented scheme is robust to the excess amplitude and phase noises of the pump field, making it a practical building block for quantum information processing and communication networks. © 2015 AIP Publishing LLC.

[<http://dx.doi.org/10.1063/1.4937569>]

For future quantum information processing and communication networks, quantum interface capable of converting quantum states between different carrier frequencies is a required building block.^{1,2} In quantum key distribution, such quantum-state-preserving frequency conversion (QFC) allows for the optimal single photon detection by converting near infrared photons to visible or near visible band photons.³ QFC can greatly facilitate the efficient connection of different quantum devices that operate at diverse optical frequencies in quantum networks,⁴ such as the connection between quantum memory devices consisting of alkaline atoms with operation wavelengths around 0.8 μm and quantum communication devices with operation wavelengths around 1.5 μm . QFC can also be employed to prepare complex multi-color entangled states where direct generation of such states are usually difficult or even impossible, due to the availability and limitation of relevant laser sources, non-linear media, or the preparation protocols.

So far, various impressive results of discrete variable QFC have been reported, including single photon and entangled photon frequency conversion employing three-wave mixing in a nonlinear crystal,^{5–16} in a cold Rb vapor,¹⁷ and four-wave mixing in a photonic crystal fiber.¹⁸ Continuous variables (CV) quantum communication and information processing protocols utilizing the degree of freedom of quadrature amplitudes of the quantized electromagnetic field have attracted great interests recently.^{19–24} By using sum-frequency generation (SFG) process, the up-conversion of nonclassical intensity correlations²⁵ and squeezed vacuum state²⁶ have been realized. The quantum frequency down-conversion of a bright amplitude-squeezed optical field via difference frequency process is also achieved recently.²⁷ At present, only QFC of single mode CV quantum states or intensity correlation between two light fields have been realized in the field of CV. However, QFC of more complex quantum states, in particular, CV

entangled states which are one of the most important resources for quantum information processing and play a pivotal role in quantum information science, has not been achieved so far.

In this letter, we propose and experimentally demonstrate a scheme to achieve robust quantum frequency up-conversion of entangled CV quantum states. The scheme is based on dual pump-enhanced SFG processes, the first one serves as the frequency conversion device of the entangled states and the other one is used for frequency conversion of the corresponding local oscillator (LO). We verify the successful entanglement transfer according to the inseparability criterion²⁸ through measuring the quantum correlations of amplitude quadrature difference and phase quadrature sum between the up-conversion beam and the remaining beam. Meanwhile, our quantum frequency conversion setup enables the preparation of entanglement between two light fields bringing approximately 1.5 octaves in optical frequency, which is the two-color entangled light field with the largest frequency span so far.

The schematic diagram of the experimental setup is depicted in Fig. 1. The initial bright two-color CV entangled light field at 806 and 1518 nm is prepared using a periodically poled KTiOPO₄ based phase-insensitive signal-injected optical parametric amplifier (for the details of the entangled source, refer to Ref. 29). The emitted signal field (entangled state) and the LO are separated by two dichroic beamsplitters (DBS) and then directed to two homodyne detectors, respectively (for simplicity, the homodyne detector at 806 nm is not shown here). The recorded quantum correlation spectra at analysis frequency of 3 MHz are plotted in Fig. 2, and the observed quantum correlations for the amplitude quadrature difference and phase quadrature sum are 3.2 dB and 3.1 dB, respectively, which satisfy the inseparability criterion for CV quantum entanglement $\langle \Delta^2(\hat{X}_{1518}^+ - \hat{X}_{806}^+) \rangle + \langle \Delta^2(\hat{X}_{1518}^- + \hat{X}_{806}^-) \rangle = 0.96 < 2$. Here, \hat{X}^+ and \hat{X}^- denote the amplitude quadrature and the phase quadrature of the light field, respectively.

In order to perform the QFC, one member of the entangled state (806 nm) and the corresponding LO beam are injected into the quantum frequency up-conversion system.

^{a)}Author to whom correspondence should be addressed. Electronic mail: yongmin@sxu.edu.cn.

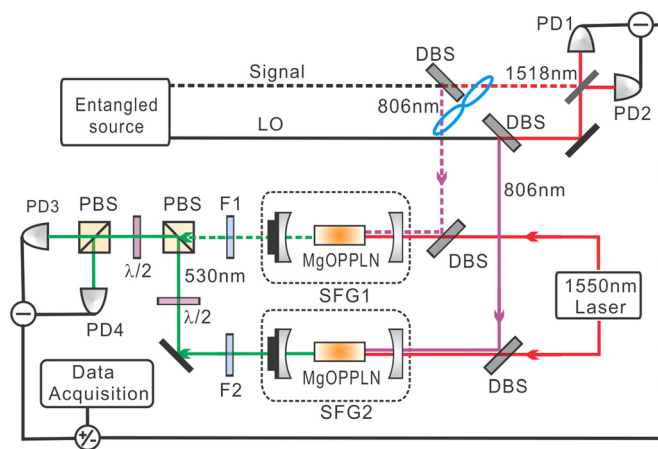


FIG. 1. Schematic of the experimental setup for quantum frequency up-conversion of continuous variable entangled states. LO, local oscillator; DBS, dichroic beamsplitter; PD1-PD4, photodetectors; PBS, polarizing beamsplitter; and F1, F2, optical filters.

The system consists of two SFG devices in which a 1 W 1550 nm single frequency fiber laser is employed as the common pump laser. Both SFG devices consist of a 30-mm-long MgO doped periodically poled lithium niobate (MgOPPLN) nonlinear crystal and two concave mirrors with 30 mm radii of curvature. Both end-faces of the MgOPPLN are anti-reflected at 1550, 806, and 530 nm, i.e., the wavelengths of pump, signal, and the up-conversion signal. The input coupler is coated for partial transmission ($\sim 4\%$) at 1550 nm and high transmission at 806 nm. The output coupler is coated for high reflectivity at 1550 nm and high transmission at both 530 and 806 nm. Such coating designs ensure a high circulating intra-cavity pump power, which is around 17 W at 350 mW pump input as well as broadband quantum frequency up-conversion process. Here, the broadband denotes that the quantum frequency converter has negligible cavity-resonance effect and actually acts as a near-ideal single-pass device for the input signal state. The bandwidth of the quantum frequency converter is a crucial parameter which

determines the effective frequency conversion range of the input quantum state during the conversion process. In our experiment, this frequency range is limited by the phase-matching bandwidth of the nonlinear crystal in principle, which is on the order of 1 nm.

After the input signal field at 806 nm and the corresponding LO are frequency up-converted through the two pump-enhanced SFG devices, the residual 806 nm and 1550 nm beams are separated from the generated 530 nm up-conversion signal field using optical filters. The filtered 530 nm up-conversion signal and LO are combined on a polarizing beamsplitter (PBS) and then interfering at a 50:50 beamsplitter consists of a half-waveplate and a PBS for further homodyne detection.

To achieve a noiseless and high fidelity quantum frequency up-conversion for bright entangled states, one must consider the excess amplitude and phase fluctuations of the pump laser which may contaminate the up-converted signal state due to the existence of the bright carrier. In the phase reference of the up-conversion LO, the dual SFG devices with the same pump source utilized here can effectively cancel the classical phase noises of the up-conversion signal field coming from the pump laser. To reduce the effect of the excess amplitude noise of pump, the pump intensity is set at the maximum conversion efficiency point. In this case, the first-order derivative of the up-conversion signal amplitude with respect to the pump field amplitude will be zero due to the conversion efficiency curve of the SFG is a smooth concave function. Therefore, the frequency up-converted quantum state will be robust to the small amplitude noises of the pump field.

When the cavity length is actively locked on resonance with the pump frequency and the temperature of the MgOPPLN is adjusted at optimal phase-matching point, the maximum classical up-conversion efficiency (photon-number conversion efficiency) for the weak 806 nm input field to the 530 nm up-conversion field is observed to be $79 \pm 1\%$. The corresponding 1550 nm pump power for the SFG1 and

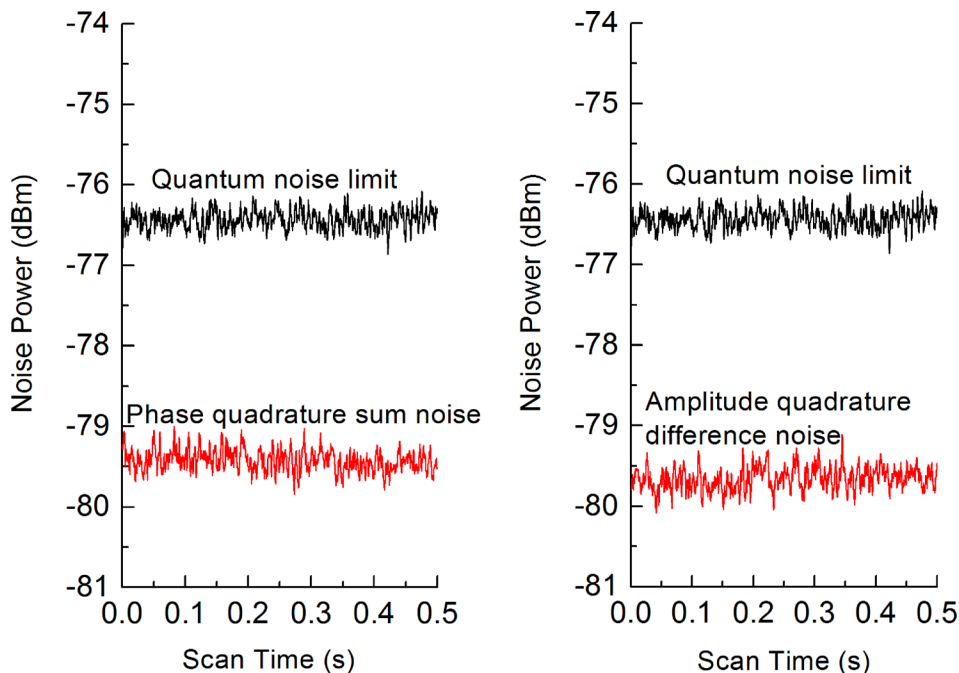


FIG. 2. Measured quadrature noise spectra for the initial 806 and 1518 nm two-color entangled state at an analysis frequency of 3 MHz. The resolution and video bandwidths of the spectrum analyzer are 300 kHz and 100 Hz, respectively.

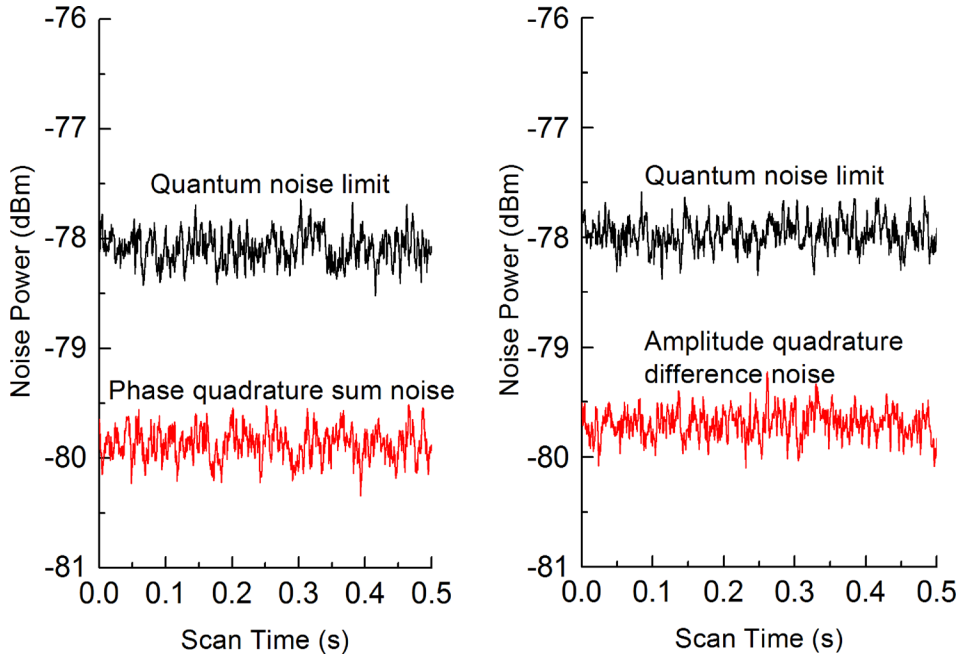


FIG. 3. Quadrature noise spectra between the up-converted 530 nm field and the remaining 1518 nm field at an analysis frequency of 3 MHz. The settings of the spectrum analyzer are the same as those in Fig. 2.

SFG2 are 370 and 390 mW, respectively. The quantum characteristics of the frequency-converted signal state are investigated by measuring the correlated quadrature noise spectra. To this end, both the 1518 nm field and the generated 530 nm field are detected by balanced homodyne detectors, and the photocurrent signals are subtracted or added and successively recorded using a spectrum analyzer.

Figure 3 illustrates the quadrature noise spectra between the 1518 nm field and up-conversion 530 nm field. The quantum noise limit (QNL) is recorded with the input signal field blocked. The phase quadrature sum noise spectrum is measured with the LO phase fixed to the phase quadrature of each signal field, while the amplitude quadrature difference noise is recorded with the LO phase fixed to the amplitude quadrature of each signal field. At an analysis frequency of 3 MHz, the observed quantum correlations for the amplitude quadrature difference and phase quadrature sum are 1.7 dB and 1.8 dB, respectively, which satisfy the inseparability criterion for CV quantum entanglement $\langle \Delta^2(\hat{X}_{1518}^+ - \hat{X}_{530}^+) \rangle + \langle \Delta^2(\hat{X}_{1518}^- + \hat{X}_{530}^-) \rangle = 1.33 < 2$. In Fig. 3, the electronic dark noises of the detectors, which are ~ 14 dB below the QNL, are not subtracted from the data. The measured correlated quadrature noise spectra prove that CV entangled states, which are more complex than CV single mode nonclassical quantum states, can be converted faithfully between different optical frequency ranges. It should be noted that our QFC setup also yields an entangled state between two light fields spanning approximately 1.5 octaves in optical frequency.

The quantum frequency up-conversion of the CV entanglement demonstrated here can be modeled with a linearized Gaussian channel with $\hat{X}_{530}^\pm = \sqrt{\eta}\hat{X}_{806}^\pm + \sqrt{1-\eta}\hat{X}_{vac}^\pm$. Here, \hat{X}_{530}^\pm , \hat{X}_{806}^\pm , and \hat{X}_{vac}^\pm are the amplitude quadratures (+) or phase quadratures (-) of the up-conversion 530 nm signal field, the input 806 nm signal field, and the vacuum field, respectively. η is the transmissivity with $\eta = \eta_T\eta_Q\eta_D$, where $\eta_T = 0.87$ is the optical propagation transmission, $\eta_Q = 0.79$ is the frequency-conversion efficiency, and $\eta_D = 0.87$ is the quantum efficiency of the photodiodes at 530 nm. Using

the following experimental values (the numbers in parentheses denote the values of phase quadrature): $\langle (\Delta\hat{X}_{1518}^\pm)^2 \rangle = 4.5$ (5.0), $\langle (\Delta\hat{X}_{806}^\pm)^2 \rangle = 5.23$ (5.6), $\langle \Delta\hat{X}_{1518}^\pm \Delta\hat{X}_{806}^\pm \rangle = 4.42$ (4.87), and $\langle \Delta^2\hat{X}_{vac}^\pm \rangle = 1$, one can obtain the theoretical quadrature noise spectra between the up-conversion 530 nm field and remaining 1518 nm field straightforwardly: $\langle [\Delta(\hat{X}_{1518}^+ - \hat{X}_{530}^+)]^2 \rangle_T = 2.4$ dB, $\langle [\Delta(\hat{X}_{1518}^- + \hat{X}_{530}^-)]^2 \rangle_T = 2.2$ dB.

The discrepancy between the theoretical prediction and the observed values ($\langle [\Delta(\hat{X}_{1518}^+ - \hat{X}_{530}^+)]^2 \rangle_E = 1.7$ dB and $\langle [\Delta(\hat{X}_{1518}^- + \hat{X}_{530}^-)]^2 \rangle_E = 1.8$ dB) is attributed mainly to the limited accuracy of phase locking between the 530 nm signal and LO due to the long propagating path before they reach the 50:50 beamsplitter. Such phase fluctuations will introduce the anti-squeezing noises and result in degradation of the observed squeezing.³⁰ The above results show that the degradation of the entanglement in our QFC is mainly due to the linear loss deriving from the optical propagation transmission and the imperfect frequency-conversion efficiency. The QFC process itself adds negligible amount of excess noise.

A perfect QFC requires that all frequency components of the input quantum states should be faithfully converted. Since any optical quantum states cover inevitably certain frequency band, especially for ultra-short pulse quantum states, which span a wide frequency range and play a key role in high speed quantum information processing. As mentioned above, the design of our scheme considers the broadband quantum frequency conversion capability, a feature crucial for a high fidelity QFC. Figure 4 shows the quadrature noise spectra from 3 MHz to 12 MHz for the initial entangled state between 806 nm and 1518 nm fields, and the frequency up-converted entangled state between 530 nm and 1518 nm fields, respectively. The observed conversion of continuous variable entangled states in a wide spectral range demonstrates the broadband conversion feature of the QFC device.

In summary, we have experimentally demonstrated quantum frequency up-conversion of continuous variable

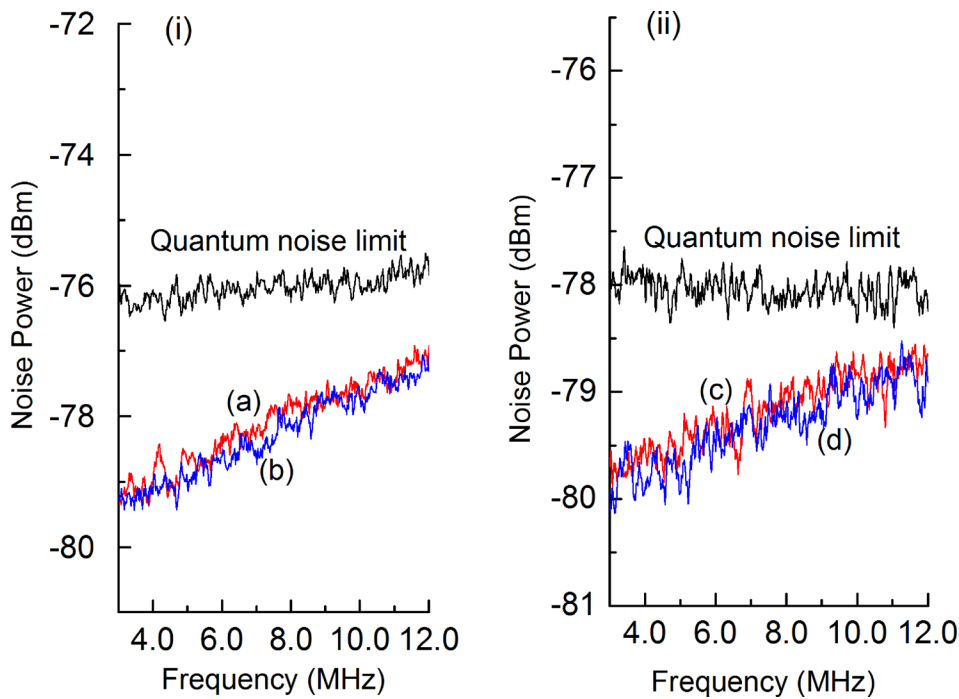


FIG. 4. Quadrature noise spectra for the initial entangled state (i) and for the frequency up-converted entangled state (ii) from 3 MHz to 12 MHz. (a) and (c) Amplitude quadrature difference noise spectrum; (b) and (d) Phase quadrature sum noise spectrum.

entangled states via efficient sum-frequency-generation process. The two-color continuous variable entangled state initially entangled in the infrared spectrum (806 and 1518 nm) is converted to a new entangled state between the visible wavelength of 530 nm and the telecommunication wavelength of 1518 nm spanning approximately 1.5 octaves in optical frequency. We thus prove that the complex continuous variable entanglement can be well preserved in sum-frequency-generation process. The scheme presented remains robust to the excess amplitude and phase noises of the pump field and is well suited for future deployment in quantum information processing and communication where quantum interface of frequency conversion of continuous variable entangled states is essential. It also opens up avenues in preparation of complex multi-color entangled states where direct generation of such states are difficult.

This research was supported by the National Natural Science Foundation of China (NSFC) (61378010), the Natural Science Foundation of Shanxi (2014011007-1), and the Program for the Outstanding Innovative Teams of Higher Learning Institutions of Shanxi.

¹S. Tanzilli, *Nature (London)* **437**, 116 (2005).

²A. P. VanDevender and P. G. Kwiat, *J. Opt. Soc. Am. B* **24**, 295 (2007).

³L. J. Ma, O. Slattery, and X. Tang, *Phys. Rep.* **521**, 69 (2012).

⁴H. J. Kimble, *Nature (London)* **453**, 1023 (2008).

⁵G. Giorgi, P. Mataloni, and F. De Martini, *Phys. Rev. Lett.* **90**, 027902 (2003).

⁶M. A. Albota, F. N. C. Wong, and J. H. Shapiro, *J. Opt. Soc. Am. B* **23**, 918 (2006).

⁷H. Takesue, *Phys. Rev. Lett.* **101**, 173901 (2008).

⁸Y. Ding and Z. Y. Ou, *Opt. Lett.* **35**, 2591 (2010).

⁹N. Curtz, R. Thew, C. Simon, N. Gisin, and H. Zbinden, *Opt. Express* **18**, 22099 (2010).

¹⁰H. Takesue, *Phys. Rev. A* **82**, 013833 (2010).

¹¹M. T. Rakher, L. J. Ma, O. Slattery, X. Tang, and K. Srinivasan, *Nat. Photonics* **4**, 786 (2010).

¹²M. T. Rakher, L. J. Ma, M. Davanço, O. Slattery, X. Tang, and K. Srinivasan, *Phys. Rev. Lett.* **107**, 083602 (2011).

¹³S. Zaske, A. Lenhard, and C. Becher, *Opt. Express* **19**, 12825 (2011).

¹⁴K. De Greve, L. Yu, P. L. McMahon *et al.*, *Nature* **491**, 421 (2012).

¹⁵C. J. McKinstrie, L. Mejlum, M. G. Raymer, and K. Rottwitz, *Phys. Rev. A* **85**, 053829 (2012).

¹⁶S. Ramelow, A. Fedrizzi, A. Poppe, N. K. Langford, and A. Zeilinger, *Phys. Rev. A* **85**, 013845 (2012).

¹⁷Y. O. Dudin, A. G. Radnaev, R. Zhao, J. Z. Blumoff, T. A. B. Kennedy, and A. Kuzmich, *Phys. Rev. Lett.* **105**, 260502 (2010).

¹⁸H. J. McGuinness, M. G. Raymer, C. J. McKinstrie, and S. Radic, *Phys. Rev. Lett.* **105**, 093604 (2010).

¹⁹C. Weedbrook, S. Pirandola, R. García-Patrón, N. J. Cerf, T. C. Ralph, J. H. Shapiro, and S. Lloyd, *Rev. Mod. Phys.* **84**, 621 (2012).

²⁰M. D. Reid, P. D. Drummond, W. P. Bowen, E. G. Cavalcanti, P. K. Lam, H. A. Bachor, U. L. Andersen, and G. Leuchs, *Rev. Mod. Phys.* **81**, 1727 (2009).

²¹T. C. Ralph and P. K. Lam, *Nat. Photonics* **3**, 671 (2009).

²²X. B. Wang, T. Hiroshima, A. Tomita, and M. Hayashi, *Phys. Rep.* **448**, 1 (2007).

²³A. Furusawa and N. Takei, *Phys. Rep.* **443**, 97 (2007).

²⁴S. L. Braunstein and P. V. Loock, *Rev. Mod. Phys.* **77**, 513 (2005).

²⁵J. M. Huang and P. Kumar, *Phys. Rev. Lett.* **68**, 2153 (1992).

²⁶C. E. Vollmer, C. Baune, A. Sambrowski, T. Eberle, V. Händchen, J. Fűrásék, and R. Schnabel, *Phys. Rev. Lett.* **112**, 073602 (2014).

²⁷D. H. Kong, Z. Y. Li, S. F. Wang, X. Y. Wang, and Y. M. Li, *Opt. Express* **22**, 24192 (2014).

²⁸L. M. Duan, G. Giedke, J. I. Cirac, and P. Zoller, *Phys. Rev. Lett.* **84**, 2722 (2000).

²⁹X. M. Guo, J. J. Zhao, and Y. M. Li, *Appl. Phys. Lett.* **100**, 091112 (2012).

³⁰Y. Takeno, M. Yukawa, H. Yonezawa, and A. Furusawa, *Opt. Express* **15**, 4321 (2007).